J Fluoresc (2014) 24:657–663
DOI 10.1007/s10895-013-1339-y

SHORT COMMUNICATION

Novel Pyrazoline-Based Selective Fluorescent Sensor for Hg^{2+}

Sheng-Qing Wang · Shu-Yan Liu · Hao-Yan Wang · Xiao-Xin Zheng · Xun Yuan · Yi-Zhi Liu · Jun-Ying Miao · Bao-Xiang Zhao

Received: 3 September 2013 / Accepted: 27 November 2013 / Published online: 13 December 2013

Abstract This paper presents the preparation of a pyrazoline compound and the properties of its UV–Vis absorption and fluorescence emission. Moreover, this compound can be used to determine Hg^{2+} ion with selectivity and sensitivity in the EtOH:H_2O=9:1 (v/v) solution. This sensor forms a 1:1 complex with Hg^{2+} and shows a fluorescent enhancement with good tolerance of other metal ions. This sensor is very sensitive with fluorometric detection limit of 3.85×10^{-10} M. In addition, the fluorescent probe has practical application in cells imaging.

Keywords Pyrazoline · Fluorescent probe · Mercury ion detection · Selective

Introduction

As a dangerous and widespread global pollutant, mercury ion can easily pass through skin, respiratory, and gastrointestinal tissues into the human body, and damage the central nervous and endocrine systems [1]. Thus, mercury pollution has sparked interest in the design of new tactics to monitor Hg^{2+} in biological and environmental samples. In the last decade, numerous scientific endeavors have focused on the development of fluorescent chemosensors for Hg^{2+} including small molecules [2–7], conjugated polymers [8, 9], nanoparticles [10–13], and biomolecules [14–16]. However, many of these systems suffer from practical use, such as cross-sensitivities toward other metal ions, narrow pH span, and delayed response, etc. Accordingly, developing new and practical, sensitive and selective chemosensor for Hg^{2+} is still a challenge.

Pyrazolines are important nitrogen containing 5-membered heterocyclic compounds with stronger fluorescence, have higher hole-transport efficiency and excellent emitting blueness property. Therefore, pyrazoline derivatives have widely been used as whitening or brightening reagents for synthetic fibers, fluorescent chemosensors for recognition of transition metal ions, hole-transport materials in the electrophotography and electroluminescence fields [17–22]. Moreover, pyrazoline with membrane permeability, low toxicity, and high quantum yield render the fluorophore attractive for biological applications [23, 24]. However, a few pyrazoline derivatives as effective "turn on" fluorescent sensors for metal ions were reported [25, 26] and only one paper presented the pyrazoline probe to detect mercury ion [27]. As an extension of our work on the development of fluorescent probe for monitoring metal ions [28–32], herein, we developed a new pyrazoline compound as a selective and sensitive fluorescent sensor for Hg^{2+} in aqueous solution. The structure of the compound was characterized by IR, ^{1}H NMR and HRMS. The association constant *K*a measured for coordination of the sensor with Hg^{2+} was 3.03×10^4 M^{-1}, and the detection limit of the sensor toward Hg^{2+} was 3.85×10^{-10} M.

Experimental Details

Apparatus

Thin-layer chromatography (TLC) was conducted on silica gel 60 F_{254} plates (Merck KGaA). ^{1}H NMR spectra were

Sheng-Qing Wang and Shu-Yan Liu with equal contribution

Electronic supplementary material The online version of this article (doi:10.1007/s10895-013-1339-y) contains supplementary material, which is available to authorized users.

S.-Q. Wang · H.-Y. Wang · X.-X. Zheng · X. Yuan · Y.-Z. Liu · B.-X. Zhao (✉)
School of Chemistry and Chemical Engineering, Shandong University, Jinan 250100, People's Republic of China
e-mail: bxzhao@sdu.edu.cn

S.-Y. Liu · J.-Y. Miao (✉)
School of Life Science, Shandong University, Jinan 250100, People's Republic of China
e-mail: miaojy@sdu.edu.cn

recorded on a Bruker Avance 300 (300 MHz) spectrometer, using DMSO-d_6 as solvent and tetramethylsilane (TMS) as internal standard. Melting points were determined on an XD-4 digital micro melting point apparatus. IR spectra were recorded with an IR spectrophotometer VERTEX 70 FT-IR (Bruker Optics). HRMS spectra were recorded on a Q-TOF6510 spectrograph (Agilent). UV–Vis spectra were recorded on a U-4100 (Hitachi). Fluorescent measurements were recorded on a Perkin-Elmer LS-55 luminescence spectrophotometer. All pH measurements were made with a Model PHS-3C pH meter (Shanghai, China) and operated at room temperature about 298 K.

Reagents

Deionized water was used throughout the experiment. All the reagents were purchased from commercial suppliers and used without further purification. The salts used in stock aqueous solutions of metal ions were $NaNO_3$, $Fe(NO_3)_3 \cdot 9H_2O$, $AgNO_3$, KNO_3, $Co(NO_3)_2 \cdot 6H_2O$, $Mg(NO_3)_2 \cdot 6H_2O$, $Ca(NO_3)_2 \cdot 4H_2O$, $Al(NO_3)_3 \cdot 9H_2O$, $Ba(NO_3)_2$, $Cr(NO_3)_3 \cdot 9H_2O$, $Ni(NO_3)_2 \cdot 6H_2O$, $Cd(NO_3)_2 \cdot 4H_2O$, $Pb(NO_3)_2$, $Cu(NO_3)_2 \cdot 3H_2O$, $Zn(NO_3)_2 \cdot 6H_2O$ and $HgCl_2$.

General Procedure for the Synthesis of Compound L

To a stirred solution of chalcone **1** (0.248 g, 1.0 mmol) and NaOH (0.116 g, 3.0 mmol) in ethanol (15 mL) was added hydrazinecarbothioamide **2** (0.116 g, 1.2 mmol). After 12 h at refluxing, the reaction mixture was allowed to cool to room temperature. Subsequently, water (30 mL) was added to the reaction mixture and the solution was neutralized with dilute hydrochloric acid. The crude product was filtrated and recrystallized with ethanol to give the products **L**, (Fig. 1) Pale Yellow solid, yield 79.8 %; mp 269–271 °C; IR (KBr, cm^{-1}): 3374.0 (N-H, st), 3265.3 (NH_2, st), 3159.9 (NH_2, st), 3060.7 (C-H, st), 2968.2 (C-H, st), 1599.9 (C=N, st), 1464.6, 1364.9 (N-H, δ); ^{1}H NMR (300 MHz, DMSO-d_6): δ 3.14 (dd, 1H, J=3.7, 18.3 Hz, 4-H_{trans}), 4.07 (dd, 1H, J=11.7, 18.3 Hz, 4-H_{cis}), 5.96 (dd, 1H, J=3.7, 11.7 Hz, 5-H of pyrazoline), 7.16–7.20 (m, 2H, Ar-H), 7.23–7.27 (m, 2H, Ar-H), 7.29–7.36 (m, 3H, Ar-H), 7.57 (d, 1H, J=7.8 Hz, NH_2), 7.68 (d, 2H, J=7.8 Hz, Ar-H), 8.38 (s, 1H, NH_2), 12.92 (s, 1H, NH); HRMS: calcd for $[M+H]^+$ $C_{17}H_{15}N_5S$: 322.1126; found: 322.1128.

Analytical Procedure

A 1.0×10^{-3} M of stock solution of compound **L** was prepared in ethanol. The cationic stocks were all in H_2O with a concentration of 10^{-1} M for UV–Vis absorption and fluorescence spectra analysis. For all measurements of fluorescence spectra, excitation was at 330 nm with 10 nm of excitation slit width and scan speed was set at 600 nm min^{-1}. UV–Vis and fluorescence titration experiments were performed using 5×10^{-5} M and 1×10^{-5} M of compound **L** in the EtOH:H_2O=9:1, respectively. For Hg^{2+} ion absorption and fluorescence titration experiments, a 3 mL solution of compound **L** (1×10^{-5} M) were filled in the quartz cell of 1 cm optical path length, and each time 1.0 μL solution of Hg^{2+} (3×10^{-3} M) were added into the quartz cell gradually by using a micro-syringe, respectively. After each addition of Hg^{2+} ion, the solution was stirred for 3 min. The volume of cationic stock solution added was less than 100 μL with the purpose of keeping the total volume of testing solution without obvious change.

Fluorescence Quantum Yield

The ability for the molecules to emit the absorbed light energy is characterized quantitatively by the fluorescence quantum yield (Φ_F). Quantum yield was determined by the relative comparison procedure, using quinine sulfate dehydrate (≥ 99.0 %) in 0.1 N H_2SO_4 as the main standard. The corrected emission spectra were measured for the quinine sulfate dehydrate standard (λ_{ex}=330 nm; A (Absorption) <0.01; Φ_F= 0.560) [33]. For all the measurements of fluorescence spectra, scan speed was 900 nm min^{-1} using a quartz cell of 1 cm optical path length. The UV–Vis absorption spectra were recorded in a standard 1 cm path length quartz cell in range 250–600 nm with spectral resolution 1 nm. The general equation used in the determination of relative quantum yields from earlier research was given in Eq. (1) [34].

$$\Phi_F = (\Phi_{FS})(F_{Au})(A_s)\left(\eta_u^2\right)/(F_{As})(A_u)\left(\eta_s^2\right) \quad (1)$$

Where Φ_F and F_A are fluorescence quantum yield and integrated area under the corrected emission spectrum, respectively; A is absorbance at the excitation wavelength; η represent the refractive index of the solution; and the subscripts u and s refer to the unknown and the standard, respectively.

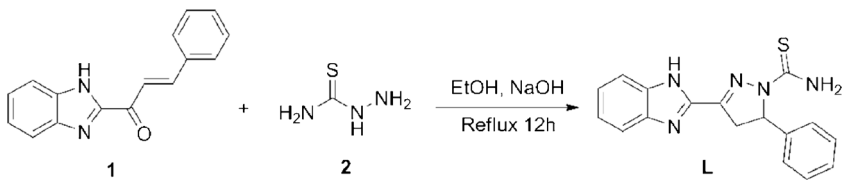

Fig. 1 Synthesis of **L**

Cell Culture and Imaging

HeLa cells were cultured in Dulbecco's modified Eagle's medium (DMEM, Gibco) containing 10 % calf bovine serum (HyClone) at 37 °C in humidified air and 5 % CO_2. For fluorescence imaging, the cells (5×10^4 mL^{-1}) were seeded into 24-well plates, and experiments to assay Hg^{2+} uptake were performed in the same media supplemented with 5, 10 or 20 μM of $Hg(ClO_4)_2$ for 1 h. The cells were washed twice with PBS buffer before staining experiments and incubated with 10 μM of the probe for 2 h in the incubator. After washing twice with PBS, the cells were imaged under a phase contrast microscope (Nikon, Japan).

Results and Discussion

Design and Synthesis of the Probe L

The synthetic route of the proposed compound **L** is outlined in Fig. 1. The starting material 1-(1*H*-benzo[d]imidazol-2-yl)-3-phenylprop-2-en-1-one was prepared according to the literature procedures [35]. The pyrazoline derivative **L** is obtained in 79.8 % yield by the reaction of chalcone **1** with hydrazinecarbothioamide **2** at reflux condition in the ethanol. As shown in Fig. S1 the structure of compound **L** was confirmed by IR, ^1H NMR and HRMS spectral data. In the IR spectra, the band at 3374.0 cm^{-1} is typical stretching vibration absorption of N-H appended to benzimidazole. Stretching vibration absorption of NH_2 peaked at 3365.3 and 3159.9. The 2 weak bands appeared at 3060.7 and 2968.2 cm^{-1} may be ascribed to the C-H absorptions. The absorption of the C=N was observed at 1599.9 cm^{-1}. Bending vibration absorption of N-H exhibited at 1364.9. In the 300 MHz ^1H NMR spectra of the compound, the CH_2 protons of the pyrazoline ring resonated as a pair of doublets at 3.14 ppm (H_d), 4.07 ppm (H_e), respectively. The CH proton at C5 also appeared as a doublet of doublets at 5.96 ppm due to vicinal coupling with the two magnetically non-equivalent protons of the methylene. The nitrogen hydrogen protons of the thioamide, respectively, presented at 7.57 and 8.38. The NH proton in the benzimidazole proton signal appeared at δ = 12.92 ppm as a single peak. HRMS showed that found $[M+H]^+$ ion peak accorded with calculated value.

Absorption Properties

The UV–Vis spectroscopic behavior of **L** toward representative metal ions was investigated by treating it with physiologically important alkali, alkaline earth, and transition metal nitrate or hydrochloride salts in aqueous 10 % ethanol solution. Sensor **L** exhibited strong absorption bands at 347 nm. Upon interaction with various metal ions, significant changes in absorption spectra were observed particularly with Hg^{2+}, Ag^+ and Cu^{2+} (Fig. S2). In the presence of mercuric ions, copper ions and silver ions the wavelength absorption peak shifts hypsochromically to 319, 292 and 317 nm, respectively.

The interaction of sensor **L** with the mercury ion was exhibited through UV–Vis spectrophotometric titration at room temperature in the HEPES buffer solution (20 mM HEPES, pH=7.2, 10 % (v/v) EtOH) (Fig. 2). Upon addition of Hg^{2+}, the absorbance decreased at 344 nm, and a new band at 314 nm increased. The isobestic point at about 328 nm was attributed to the equilibrium between the receptor **L** and Hg^{2+} throughout

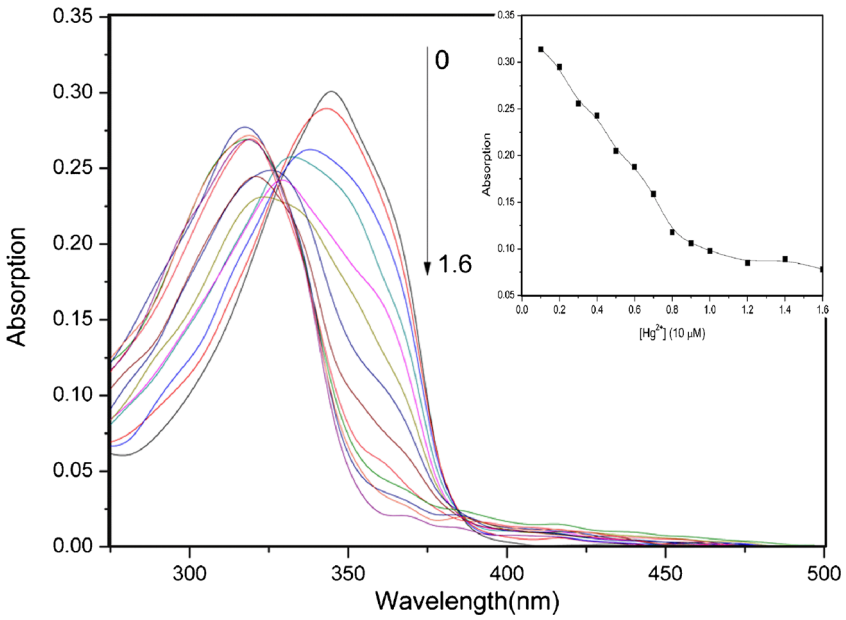

Fig. 2 Absorption spectra of **L** (10 μM) upon the addition of Hg^{2+} (0–6.0 equiv.) in buffered EtOH:HEPES=9:1 solution at pH 7.2. Insert: Absorption changes of the sensor **L** at 344 nm upon the addition of Hg^{2+} (0–6.0 equiv.)

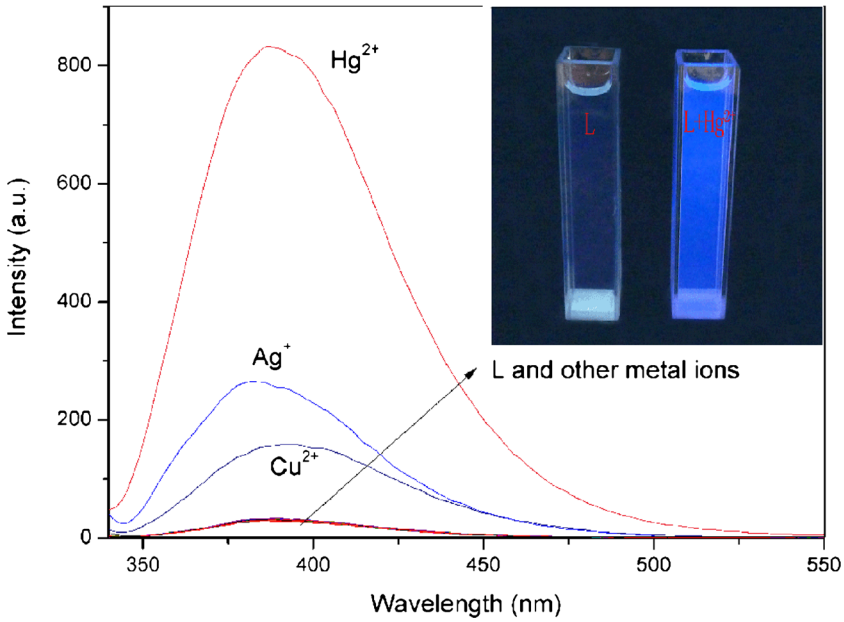

Fig. 3 Fluorescence spectra of **L** (10 μM) upon addition of various metal ions (100 μM) in buffered EtOH:HEPES=9:1 solution at pH 7.2 under 1 % attenuation (excitation at 330 nm). Inset: Photograph of compound **L** in the HEPES buffer (20 mM HEPES, pH=7.2, EtOH:HEPES=9:1) without (*left*) and with (*right*) addition of 100 μM Hg^{2+} ion under the irradiation of UV light at 365 nm

the titration process. By plotting the changes of receptor **L** in the absorbance at 344 nm as a function of Hg^{2+} concentration, nonlinear curve was obtained and is shown in the inset of Fig. 3. Based on a Job plot analysis, the receptor L : Hg^{2+} ion ratio was found to be 1:1.

Selectivity Studies

We monitored the fluorescence change after adding various metal cations to examine the selectivity of the sensor for Hg^{2+} ions. As shown in Fig. 3, the sensor **L** showed a very weak fluorescence centered around 390 nm in EtOH-HEPES buffer (20 mM HEPES, pH=7.2, EtOH:HEPES=9:1) under 1 % attenuation (exCitation at 330 nm). Upon interaction with, Cd^{2+}, Pb^{2+}, Na^{+}, K^{+}, Ca^{2+}, Mg^{2+}, Ni^{2+}, Zn^{2+}, Ba^{2+}, Hg^{2+}, Cu^{2+}, Co^{2+}, Cr^{3+}, Ag^{+}, Al^{3+} and Fe^{3+}, the effect of selected ions on the intensity of sensor **L** showed a low interference except Cu^{2+}, Ag^{+} and Hg^{2+} ions. As large as 26-fold "off-on" type fluorescence enhancement was observed upon the addition of Hg^{2+}, while its homologues Cu^{2+} and Ag^{+} showed a 5- and 8-fold enhancement only under the same conditions. The effects of other common metal ions on the Hg^{2+} signaling of **L** were also assessed under competitive conditions (Fig. 4). The fluorescence increase was not significantly affected by the presence of other metal ions at 5 equiv, except for Cu^{2+}, Ag^{+}, Cd^{2+} and Fe^{3+}. Therefore, these results suggest that **L**

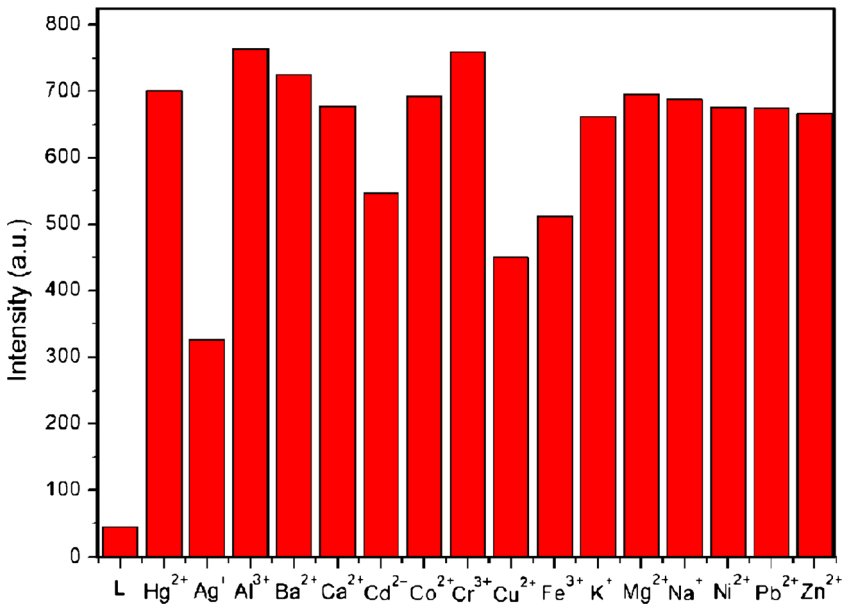

Fig. 4 Fluorescence spectra of **L** + Hg^{2+} system in the presence of possibly interfering metal ions as background in buffered EtOH: HEPES=9:1 solution at pH 7.2 under 1 % attenuation [**L**]=1×10^{-5} M, [Hg^{2+}]=5.0×10^{-5} M, [M^{n+}]=5.0×10^{-5} M, λ_{ex}=330 nm (I at 388 nm)

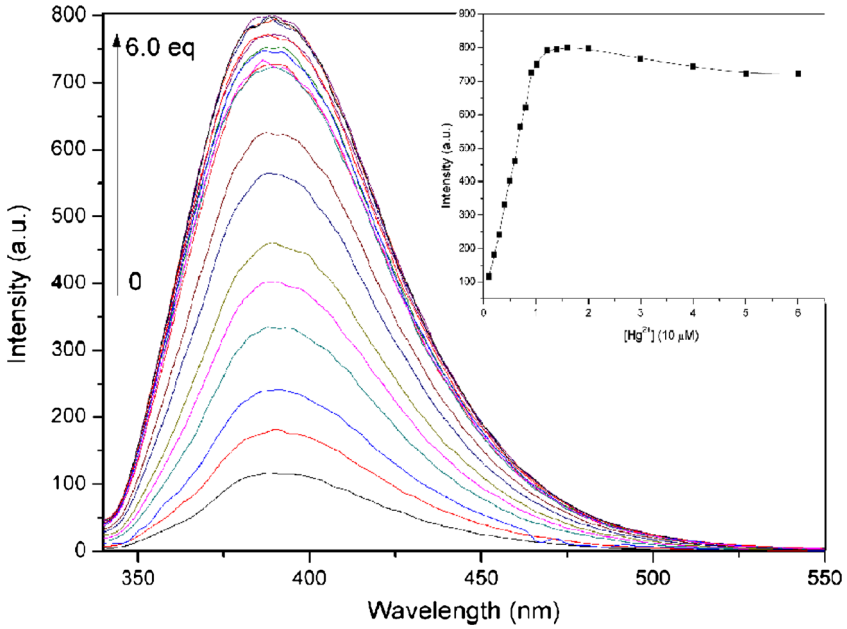

Fig. 5 Fluorescence emission spectra of **L** (10 μM) in buffered EtOH:HEPES=9:1 solution at pH 7.2 under 1 % attenuation upon the addition of Hg^{2+} (0–6.0 equiv.). Excitation wavelength was 330 nm. Inset: variations of fluorescence intensity of compound **L** (10^{-5} M) at 388 nm vs. equivalents of [Hg^{2+}]

has a high fluorescent selectivity for Hg^{2+} in the presence of these tested foreign metal ions.

Hg^{2+}-Titration

The fluorescence titration of **L** in the presence of different Hg^{2+} concentrations was then performed in buffered EtOH:HEPES=9:1 solution at pH 7.2 under 1 % attenuation. As shown in Fig. 5, the sensor emits weak fluorescence at 388 nm. As the concentration of Hg^{2+} ion is increased in the solution of **L** (maximum 6 equiv.), the intensity of emission band at 388 nm was gradually enhanced and almost reached maximum when the amount of Hg^{2+} ion was about 10 μM. When more $HgCl_2$ solution was titrated, the fluorescence

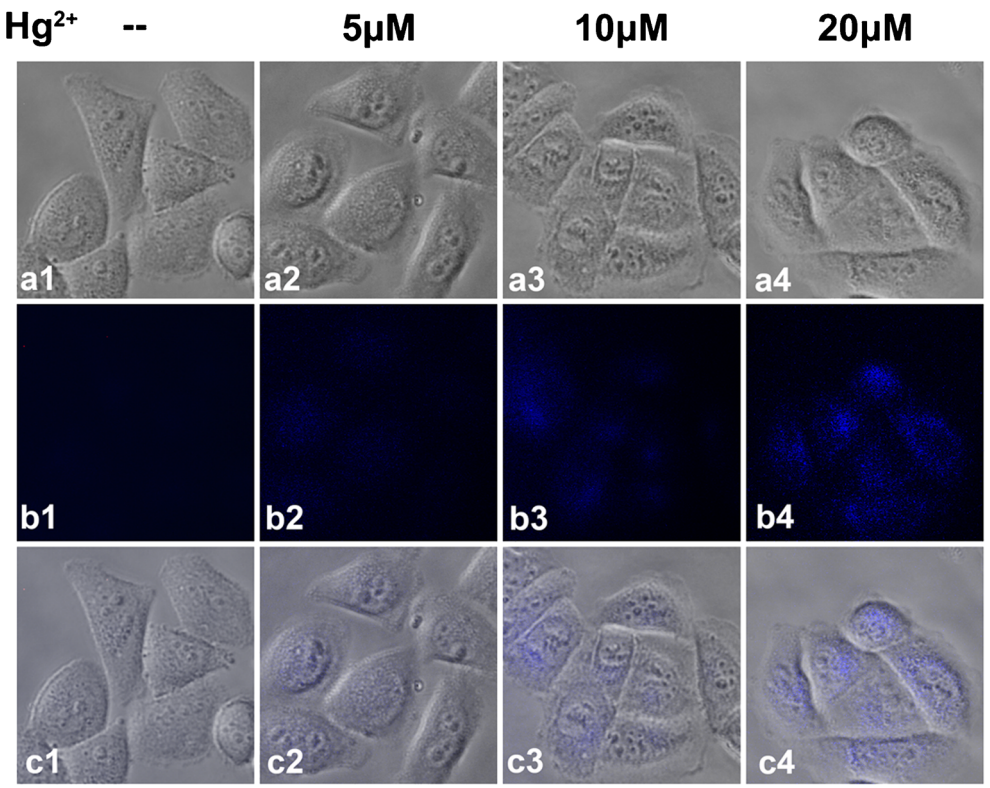

Fig. 6 Fluorescence images of living HeLa cells. (a1–4): Bright-field view of panel; (b1–4): Fluorescent; (c1–4): Overlay image of (a1–4) and (b1–4). 1: Cells incubated with 10 μM of the sensor for 2 h at 37 °C. 2, 3 and 4: HeLa cells were pretreated with Hg^{2+} at the indicated concentrations for 1 h at 37 °C before incubating with the probe under the same conditions

intensity showed negligible changes and the curve (inset) remained relatively constant, which also gives a 1:1 stoichiometric ratio between sensor **L** and Hg^{2+} similar to Job's plot in Fig. S3. The fluorescence quantum yield increases from 0.0465 for free **L** to 0.8593 for the complex of **L** and Hg^{2+}, correspondingly. In addition, the quantitative response of the sensor **L** toward Hg^{2+} ion was also studied by the fluorescence titration and the linear calibration plots as shown in Figs. S4 and S5. The dynamic range for the determination of Hg^{2}+ was determined to be linear in the range of 0–10 μM with correlation coefficient (R) of 0.9949 [36]. The limit of detection (LOD) is evaluated using $3\sigma_{bi}/m$ [37], where σbi is the standard deviation of the blank signals and m is the slope of the linear calibration plot. The LOD for determination of Hg^{2+} was thus calculated to be 3.85×10^{-10} M, a value superior to those reported to date. Following a Benesi-Hildebrand-type analysis [38], the association constant *K*a was determined to be 3.03×10^{4} M^{-1}.

Binding of Probe L with Hg^{2+}

In an effort to gain more detailed information on the interactions between **L** and Hg^{2+} ion, ^{1}H NMR spectroscopic studies were carried out in DMSO-d_6, and the spectral differences are shown in Fig. S7. A distinct change occurs at the peak centered at 8.38 and 7.57 ppm, Hb and the Hc proton proximal to the thioamide are shifted downfield by 1.0 ppm and 1.18 ppm, respectively, with the stepwise addition of Hg^{2+} ions. The single peak assigned for the Ha proton of the N-H in the benzimidazole experiences a slight net downfield shift from 12.92 to 13.01 ppm. Moreover, the proton Hd and the He proton to the CH_2 protons of the pyrazoline ring are shifted downfield by 0.21 ppm and 0.22 ppm, respectively. These observations suggested that the nitrogen atoms in the benzimidazole, thioamide and pyrazoline of the sensor **L** participated to the complex with Hg^{2+}. A proposed binding mode is shown in Fig. S8.

Reversibility and Effect of pH

Fluorescence intensity changes of the sensor **L** as a function of pH in the presence and absence of Hg^{2+} ion are also noticeable (Fig. S8). We found that in buffered EtOH: HEPES=9:1 solution at pH 7.2 under 1 % attenuation the suitable pH span for Hg^{2+} determination is between pH 7 and pH 11. In this region, the free **L** has no response, while addition of Hg^{2+} ion can lead to a remarkable response; suggesting efficient complexation between the sensor and Hg^{2+} ion. As a result, our Hg^{2+}-selective receptors would be an ideal chemosensor for monitoring Hg^{2+} in aqueous solution in the pH range of 7–11.

Imaging of Intracellular Hg^{2+}

The intracellular Hg^{2+} imaging behaviour of **L** was carried out on HeLa cells by a fluorescence microscope (Fig. 6). Incubation of HeLa cells with 10 μM of the sensor for 2 h at 37 °C gave almost no intracellular fluorescence. This was consistent with the previous findings that cancer cells in cell cultures contain little Hg^{2+}. When HeLa cells were pretreated with 5 μM of Hg^{2+}, fluorescence is visible in the HeLa cells with the same treatment with the sensor, providing visual evidence of the sensor permeating cells and information on the intracellular existence of Hg^{2+}. Furthermore, when pretreated with 10, 20 μM of Hg^{2+}, fluorescence images of the cells revealed a remarkable enhancement of intracellular fluorescence. It is proved that the sensor can be used for monitoring Hg^{2+} within biological samples.

Conclusions

In summary, a new highly selective and sensitive fluorescent sensor based on pyrazoline unit was synthesized and used for the determination of Hg^{2+} ion with a low detection limit in buffered EtOH:HEPES=9:1 solution at pH 7.2. This sensor formed a 1:1 complex with Hg^{2+} and showed a fluorescent enhancement with good tolerance of other metal ions. The fluorometric detection limit of 3.85×10^{-10} M of this seneor is superior to one reported up to date. Moreover, the fluorescent sensor has practical application in cell imaging.

Acknowledgements This study was supported by 973 Program (2010CB933504).

References

1. US EPA, (2005) Regulatory impact analysis of the clean air mercury rule: EPA-452/R-05-003.
2. Nolan EM, Lippard SJ (2008) Tools and tactics for the optical detection of mercuric ion. Chem Rev 108:3443–3480
3. Khan TK, Ravikanth M (2012) 3-(Pyridine-4-thione)BODIPY as a chemodosimeter for detection of Hg(II) ions. Dyes Pigments 95:89–95
4. Pal A, Bag B (2012) Hg(II) ion specific dual mode signalling in a thiophene derivatized rhodamine based probe and their complexation cooperativity. J Photoch Photobio A 240:42–49
5. Kumar M, Kumar N, Bhalla V (2012) Rhodamine appended thiacalix[4]arene of 1,3-alternate conformation for nanomolar detection of Hg^{2+} ions. Sensor Actuat B 161:311–316
6. Guo XR, Li B, Zhang LM, Wang YH (2012) Highly selective fluorescent chemosensor for detecting Hg(II) in water based on pyrene functionalized core-shell structured mesoporous silica. J Lumin 132:1729–1734
7. Quang DT, Kim JS (2010) Fluoro- and chromogenic chemodosimeters for heavy metal ion detection in solution and biospecimens. Chem Rev 110:6280–6301

8. Yang B, Li GZ, Zhang X, Shu X, Wang AN, Zhu XQ, Zhu J (2011) Hg^{2+} detection by aniline-based conjugated copolymers with high selectivity. Polymer 52:2537–2541
9. Saha S, Chhatbar MU, Mahato P, Praveen L, Siddhanta AK, Das A (2012) Rhodamine-alginate conjugate as self indicating gel beads for efficient detection and scavenging of Hg^{2+} and Cr^{3+} in aqueous mediaw. Chem Commun 48:1659–1661
10. Li F, Wang J, Lai YM, Wu C, Sun SQ, He YH, Ma H (2013) Ultrasensitive and selective detection of copper(II) and mercury(II) ions by dye-coded silver nanoparticle-based SERS probes. Biosens Bioelectron 39:82–87
11. Wang CI, Huang CC, Lin YW, Chen WT, Chang HT (2012) Catalytic gold nanoparticles for fluorescent detection of mercury(II) and lead(II) ions. Anal Chim Acta 745:124–130
12. Roy B, Bairi P, Nandi AK (2011) Selective colorimetric sensing of mercury(II) using turn off-turn on mechanism from riboflavin stabilized silver nanoparticles in aqueous medium. Analyst (Cambridge, U K) 136:3605–3607
13. Liu BY, Zeng F, Wu GF, Wu SZ (2012) Nanoparticles as scaffolds for FRET-based ratiometric detection of mercury ions in water with QDs as donors. Analyst (Cambridge, U K) 137:3717–3724
14. Fan J, Chen C, Lin Q, Fu NY (2012) A fluorescent probe for the dual-channel detection of Hg^{2+}/Ag^{+} and its Hg^{2+}-based complex for detection of mercapto biomolecules with a tunable measuring range. Sensor Actuat B 173:874–881
15. Li M, Zhou XJ, Ding WQ, Guo SW, Wu NQ (2013) Fluorescent aptamer-functionalized graphene oxide biosensor for label-free detection of mercury(II). Biosens Bioelectron 41:889–893
16. Wu JS, Sheng RL, Liu WM, Wang PF, Ma JJ, Zhang HY, Zhuang XQ (2011) Reversible fluorescent probe for highly selective and sensitive detection of mercapto biomolecules. Inorg Chem 50:6543–6551
17. Gong ZL, Zhao BX, Liu WY, Lv HS (2011) A new highly selective "turn on" fluorescent sensor for zinc ion based on a pyrazoline derivative. J Photoch Photobio A 218:6–10
18. Gong ZL, Ge F, Zhao BX (2011) Novel pyrazoline-based selective fluorescent sensor for Zn^{2+} in aqueous media. Sensor Actuat B 159: 148–153
19. Gong ZL, Xie YS, Zhao BX, Lv HS, Liu WY, Zheng LW, Lian S (2011) The synthesis, X-ray crystal structure and optical properties of novel 5-aryl-3-ferrocenyl-1-pyridazinyl-pyrazoline derivatives. J Fluoresc 21:355–364
20. Gong ZL, Zheng LW, Zhao BX, Yang DZ, Lv HS, Liu WY, Lian S (2010) The synthesis, X-ray crystal structure and optical properties of novel 1,3,5-triaryl pyrazoline derivatives. J Photoch Photobio A 209: 49–55
21. Liu WY, Xie YS, Zhao BX, Wang BS, Lv HS, Gong ZL, Lian S, Zheng LW (2010) The synthesis, X-ray crystal structure and optical properties of novel 5-aryl-1-arylthiazolyl-3-ferrocenyl-pyrazoline derivatives. J Photoch Photobio A 214:135–144
22. Gong ZL, Zheng LW, Zhao BX (2012) Synthesis, X-ray crystal structure and optical properties research of novel diphenyl sulfone-based bis-pyrazoline derivatives. J Lumin 132:318–324
23. Li JF, Li DX, Han YY, Shuang SM, Dong C (2009) Synthesis of 1-phenyl-3-biphenyl-5-(N-ethylcarbazole-3-yl)-2-pyrazoline and its use as DNA probe. Spectrochim Acta A 73:221–225
24. Fahrni CJ, Yang LC, VanDerveer DG (2003) Tuning the photoinduced electron-transfer thermodynamics in 1,3,5-Triaryl-2-pyrazoline fluorophores: X-ray structures, photophysical characterization, computational analysis, and in vivo evaluation. J Am Chem Soc 125:3799–3812
25. Ciupa A, Mahon MF, Bank PAD, Caggiano L (2012) Simple pyrazoline and pyrazole "turn on" fluorescent sensors selective for Cd^{2+} and Zn^{2+} in MeCN. Org Biomol Chem 10:8753–8757
26. Zhang Z, Wang FW, Wang SQ, Ge F, Zhao BX, Miao JY (2012) A highly sensitive fluorescent probe based on simple pyrazoline for Zn^{2+} in living neuron cells. Org Biomol Chem 10:8640–8644
27. Rurack K, Resch-Genger U, Bricksb JL, Spieles M (2000) Cation-triggered 'switching on' of the red/near infra-red (NIR) fluorescence of rigid fluorophore-spacer-receptor ionophores. Chem Commun 36:2103–2104
28. Liu WY, Li HY, Zhao BX, Miao JY (2012) A new fluorescent and colorimetric probe for Cu^{2+} in live cells. Analyst (Cambridge, U K) 137:3466–3469
29. Liu WY, Li HY, Zhao BX, Miao JY (2011) Synthesis, crystal structure and living cell imaging of a Cu^{2+}-specific molecular probe. Org Biomol Chem 9:4802–4805
30. Liu WY, Li HY, Lv HS, Zhao BX, Miao JY (2012) A rhodamine chromene-based turn-on fluorescence probe for selectively imaging Cu^{2+} in living cell. Spectrochim Acta A 95:658–663
31. Wang SQ, Gao Y, Wang HY, Zheng XX, Shen SL, Zhang YR, Zhao BX (2013) Synthesis, X-ray crystal structure and optical properties of novel 1,3,5-triarylpyrazoline derivatives and the fluorescent sensor for Cu^{2+}. Spectrochim Acta A 106:110–117
32. Jiang ZJ, Lv HS, Zhu J, Zhao BX (2012) New fluorescent chemosensor based on quinoline and coumarine for Cu^{2+}. Synthetic Met 162:2112–2116
33. Velapoldi RA, Mielenz KD (1980) A fluorescence standard reference material: quinine sulfate dihydrate. National Bureau of Standards (now the National Institute of Standards and Technology, NIST). Special Publication, Washington DC, pp 260–264
34. Song SM, Ju D, Li JF, Li DX, Wei YL, Dong C, Lin PH, Shuang SM (2009) Synthesis and spectral characteristics of two novel intramolecular charge transfer fluorescent dyes. Talanta 77:1707–1714
35. Reddy VM, Reddy KR (2010) Synthesis and biological evaluation of some novel-3-(5-substitutedbenzimidazol-2-yl)-5-arylisoxazolines. Chinese Chem Lett 21:1145–1148
36. Li N, Xiang Y, Chen XT, Tong AJ (2009) Salicylaldehyde hydrazones as fluorescent probes for zinc ion in aqueous solution of physiological pH. Talanta 79:327–332
37. Joshi BP, Park J, Lee WI, Lee KH (2009) Ratiometric and turn-on monitoring for heavy and transition metal ions in aqueous solution with a fluorescent peptide sensor. Talanta 78:903–909
38. Yuan MJ, Zhou WD, Liu XF, Zhu M, Li JB, Yin XD, Zheng HY, Zuo ZC, Ouyang CB, Liu HB, Li YL, Zhu DB (2008) A multianalyte chemosensor on a single molecule: promising structure for an integrated logic gate. J Org Chem 73:5008–5014